Development of an Exoskeleton type Manta Ray Robot

Takumi Asada[1], Tatsunari Tsujimoto[2], Hideo Furuhashi[3]
[1]Graduate School of Engineering, Aitch Institute of Technology, Japan
tasada381@gmail.com
[2]Graduate School of Engineering, Aitch Institute of Technology, Japan
tatsunari.tsujimoto0523@gmail.com
[3]Department of Electrical and Electronics Engineering, Aitch Institute of Technology, Japan
furuhasi@aitech.ac.jp

1 Introduction

The oceans cover approximately two-thirds of the Earth, and underwater robots are growing in demand for surveying underwater structures and petroleum [1, 2]. Several biomimetic robots that differ from conventional propulsion methods have been developed. The robot is used to conduct surveys of the marine environment [3]. The robot has more advantages in the water, such as high efficiency, high mobility and low noise [4, 5].

The swimming locomotion of fish can be classified into two types based on the propulsion mode: body and caudal fin (BCF) mode and median or paired fin (MPF) mode. BCF fish have superior propulsion and acceleration, whereas MPF fish have higher efficiency and mobility at low speed [6]. In the MPF, manta rays have high turning performance and mobility owing to their large pectoral fins. Manta rays propel themselves by bending their wings and pushing the water [7]. Therefore, manta ray robots have been developed with a distributed multistage skeletal structure and soft materials [5,8]. Bending is achieved in soft material robots by soft fins. In the distributed multi-stage skeletal structure, bending is achieved by changing the amplitude and phase difference of each skeleton. However, soft fins are affected by water pressure, shape changes, and deterioration. It is difficult to operate in water owing to the change in volume caused by transformation. Each skeleton has a simple trajectory in a distributed multistage skeletal structure. This skeleton is propelled in multistage to realize a sinusoidal wave. However, this motion trajectory is different from the actual manta rays.

To overcome the disadvantages of the soft fins, the robot developed in this study has a completely rigid body. Long-term operation is possible owing to the inability to readily change the robot's shape. In addition, the structure of each wing uses three joints with inclined rotational axis to realize the distortion with rigid wings. This realizes the motion trajectory of an actual manta ray, and efficient swimming.

2 Developed Robot

According to Fish *et al.* [9], the amplitudes and periods of the upstroke and downstroke of the manta ray are different. The asymmetrical motion causes wing bending and distortion, resulting in a large propulsive force.

To achieve this bending and distortion with a rigid wing, the robot was developed by dividing the wings into three triangles with the same origin. Figures 1(a) and (b) show the developed robot and bending model, respectively. The center of gravities for each wing section are ${}^1C_1$, ${}^2C_2$, and ${}^3C_3$, respectively. The inclinations of the rotational axis connecting each section are Φ_1, Φ_2, and Φ_3, respectively. The specifications are listed in Table 1.

When the wing moves in an actual manta ray, it is bent and distorted by the water pressure. A spring-damper system was used to model the wing motion. The joints were numbered as 1, 2, and 3 in the order of the root to the wing tip. Joint 1 is assumed to exactly follow the target angle. Equation (1) expresses motion for Joints 2 and 3:

$$\begin{aligned} \boldsymbol{k_2 \Delta\theta_2 + \tau_2 = 0,} \\ \boldsymbol{k_3 \Delta\theta_3 + \tau_3 = 0,} \end{aligned} \tag{1}$$

where $\Delta\theta_2$ and $\Delta\theta_3$ are the differences between the target angle and the bend angle of joints 2 and 3, respectively. τ_2 and τ_3 represent the damper damping forces of joints 2 and

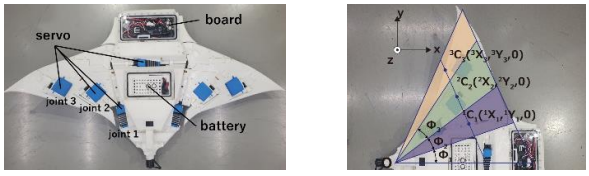

(a) (b)

Figure 1: Exoskeleton type manta ray robot. (a) Overall structure; (b) Detailed structural diagram of bending model.

Table 1 Specifications of the manta ray robot.

Items	Characteristics
Dimension (L×W×H)	0.45 [m]×0.80 [m] ×0.10 [m]
Weight	3.9 [kg]
Control method	Wireless remote control
Power supply	Li-Po battery 7.4 [V]

3, respectively, and are proportional to the velocity of each section. k_2 and k_3 represent the spring constants of joints 2 and 3, respectively, which correspond to the elasticity of the wing. The equations for the angular velocities were obtained by solving Eq.(1) with the kinematics of the structure shown in Figure 1 (b). The wing angles were calculated and the actuators were sequentially controlled. Changing the target angle of each joint $\theta_{1target}$, $\theta_{2target}$, and $\theta_{3target}$ as shown in Eq. (2).

$$\begin{aligned} \boldsymbol{\theta_{1target} = \theta_{1max} \sin \omega t} \\ \boldsymbol{\theta_{2target} = \theta_{2max} \sin \omega t} \\ \boldsymbol{\theta_{3target} = \theta_{3max} \sin \omega t} \end{aligned} \quad (2)$$

The parameter of θ_{1max}, θ_{2max}, θ_{3max} are the maximum joint angle.

3 Experiment

3.1 Method

It was verified that the modeled motion could achieve the actual manta trajectory and bending. The amplitude trajectory of each joint was tracked using markers placed on each section of a wing. They were defined as P1, P3, and P5, starting from the root of the wing.

Additionally, the usefulness of the bending model was verified by measuring the velocity in an experimental pool. The experiments were conducted in an outdoor pool with a diameter of 4.5 m. A motion capture system OptiTrack (NaturalPoint Inc.) was used for the measurements.

3.2 Results and Discussions

Figure 3 shows the tracking snapshot series of the amplitude trajectories. Figure 4 shows the trajectories of the tracking markers. As the amplitude increased, the phase delayed from the root to the wing tip.

Figures 5 and 6 show the swimming snapshot series and the trajectory, respectively. A straight swimming velocity of 0.135 [m/s] was obtained.

The rigid wing divided by three triangles was useful to realize the manta ray motion.

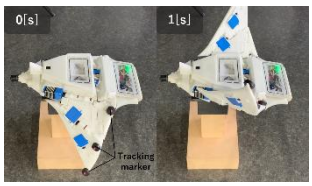

Figure 3: Tracking snapshot series.

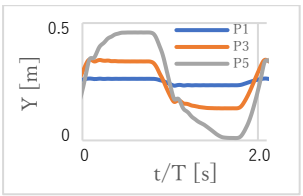

Figure 4: Trajectories of the tracking markers.

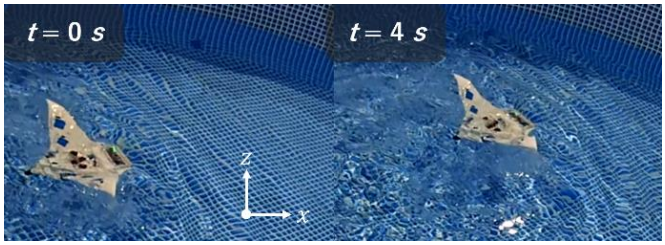

Figure 5: Swimming snapshot series.

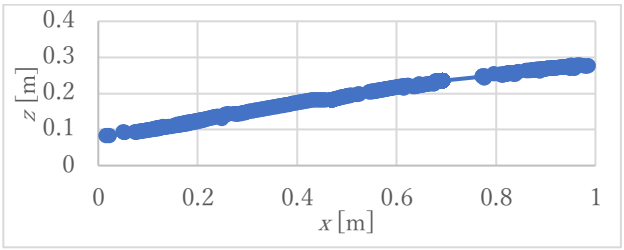

Figure 6: Swimming trajectory.

4 Conclusion

In this study, an exoskeletal manta ray robot that achieved bending with three joints with inclined rotational axis and three wing sections was developed. The rigid body enabled long-term operation without transformation. A bending model of manta rays was proposed, and the effectiveness of the model was confirmed. A swimming velocity of 0.135[m/s] was obtained using the bending model.

References

[1] J.Yuh, "Design and Control of Autonomous Underwater Robots: A Survey," *Autonomous Robots*, Vol.8, pp.7-24, 2000.

[2] H. I. Moud, A. Shojaei, I. Flood, "Current and Future Applications of Unmanned Surface, Underwater and Ground Vehicles in Construction," Construction Research Congress, 2018.

[3] R. K. Katzschmann, J. DelPreto, R. MacCurdy, D. Rus, "Exploration of Underwater Life with an Acoustically Controlled Soft Robotic Fish," Science Robotics, Vol.3, No.16, 2018.

[4] M. S. Triantafyllou, and G. S. Triantafyllou, "An Efficient Swimming Machine," *Scientific America*, Vol.272, No.3, pp.64-70, 1995.

[5] G. Liu, Y. Ren, J. Zhu, H. Bart-Smith, and H. Dong, "Thrust Producing Mechanisms in Ray-inspired Underwater Vehicle Propulsion," *Theoretical and Applied mechanics letters*, Vol.5, No.1, pp.54-57, 2015.

[6] M. Sfakiotakis, J. Bruce, C. Davies, and D. M. Lane, "Review of Fish Swimming Modes for Aquatic Locomotion," *IEEE Journal of Oceanic Engineering*, Vol. 24, No. 2, pp.237-252, 1999.

[7] F. E. Fish, A. Crossett, M. A. Dudas, K. W. Moored, and H. Bart-Smith, "Kinematics of Swimming of the Manta Ray: Three-dimensional Analysis of Open-water Maneuverability," *Journal of Experimental Biology*, Vol.221, No. 6, 2018, doi:10.1242/jeb.166041.

[8] Y. Cao, Y. Xie, Y. He, G. Pan, Q. Huang, and Y. Cao, "Bioinspired Central Pattern Generator and T-S Fuzzy Neural Network-Based Control of a Robotic Manta for Depth and Heading Tracking," *Journal of Marine Science and Engineering*, Vol. 10, No. 6, pp.758, 2022.

[9] F. E. Fish, C.M. Schreiber, K. W. Moored, G. Liu, H. Dong, and H. Bart-Smith, "Hydrodynamic, Performance of Aquatic Flapping: Efficiency of Underwater Flight in the Manta," Aerospace, Vol. 3, No. 3, pp.30, 2016.